

## EXPERIMENTAL RACETRACK SHAPED JET IMPINGEMENT ON A ROUGHENED LEADING-EDGE WALL WITH FILM HOLES

by

**M.E. Taslim , Y. Pan and K. Bakhtari**

Mechanical, Industrial and Manufacturing Engineering  
 Northeastern University  
 Boston, Massachusetts  
 USA

### ABSTRACT

Compatible with the external contour of the turbine airfoils at their leading edge, the leading-edge cooling cavities have a complex cross-sectional shape. To enhance the heat transfer coefficient on the leading-edge wall of these cavities, the cooling flow in some designs enters the leading-edge cavity from the adjacent cavity through a series of crossover holes on the partition wall between the two cavities. The crossover jets then impinge on the concave leading-edge wall and exit through the showerhead film holes, gill film holes on the pressure and suction sides, and, in some cases, form a crossflow in the leading-edge cavity and move toward the airfoil tip. The main objective of this investigation was to study the effects that racetrack crossover jets, in the presence of film holes on the target surface, have on the impingement heat transfer coefficient. Available data in open literature are mostly for impingement on a flat smooth surface with no representation of the film holes. This investigation covered new features in airfoil leading-edge cooling concept such as impingement with racetrack shaped holes on a roughened target surface with a row of holes representing the leading-edge showerhead film holes. Results of the circular crossover jets impinging on these leading-edge surface geometries with and without showerhead holes were reported by these authors previously. In this paper, however, the experimental results are presented for the impingement of racetrack-shaped crossover jets on a concave surface with showerhead film holes. The investigated target surface geometries were : (1) a smooth wall, (2) a wall roughened with big conical bumps, (3) a wall roughened with smaller conical bumps and (4) a wall roughened with tapered radial ribs. The tests were run for a range of flow arrangements and jet Reynolds numbers and the results were compared with those of round crossover jets. The major conclusions of this

study are: (a) for a given jet Reynolds number, the racetrack crossover jets produce a higher impingement heat transfer coefficient than the circular jets, (b) the overall heat transfer performance of  $0^\circ$  racetrack crossover jets is superior to that of  $45^\circ$  racetrack crossover jets and (c) there is a heat transfer enhancement benefit in roughening the target surface. With the presence of showerhead holes, the enhancement is due to both the impingement heat transfer coefficient and the heat transfer area increase.

### NOMENCLATURE

$A_{base}$	leading-edge base area for the smooth case
$A_{hole}$	total area of all nine cross-over holes
$A_{HT}$	total heat transfer area including the surface roughness
$AR$	cooling channel aspect ratio
$AR_{rib}$	rib aspect ratio
$d_{gill}$	gill hole diameter (0.488 cm)
$d_{jet}$	racetrack hole hydraulic diameter (0.921 cm)
$d_{shower}$	showerhead hole diameter (0.38 cm)
$D_h$	cooling channel hydraulic diameter
$e$	roughness height
$h$	average heat transfer coefficient on the leading-edge wall, $[(vi/A_{HT}) - q_{loss}]/(T_s - T_{jet})$
$i$	current through the foil heater on the middle brass piece
$k$	air thermal conductivity
$m$	total mass flow rate through all nine crossover holes
$Nu_{jet}$	average Nusselt number based on the jet diameter, $hd_{jet}/k$

$P$	channel perimeter without ribs
$P_{feed}$	supply channel pressure
$P_{LE}$	leading-edge channel pressure
$q_{loss}$	heat losses from the middle brass piece to the ambient by conduction and convection as well as the heat losses by radiation to the unheated walls
$R_{nose}$	channel radius at the leading edge
$Re_{jet}$	Reynolds number based on the jet diameter ( $\rho U_{jet} d_{jet} / \mu$ )
$S$	Rib pitch
$T_{jet}$	air jet temperature
$T_s$	surface temperature
$U_{jet}$	jet mean velocity, $m/pA_{hole}$
$Z$	jet place distance to the target surface (Figure 1)
$v$	voltage drop across the foil heater on the middle brass piece
$\alpha$	rib angle of attack
$\beta$	showerhead hole angle with the channel axial direction ( $30^\circ$ , Figure 1)
$\gamma$	racetrack hole angle with the leading-edge channel axis ( $0^\circ$ and $45^\circ$ , Figure 2e)
$\mu$	air dynamic viscosity at jet temperature
$\rho$	air density at jet temperature and pressure

## INTRODUCTION

Various methods have been developed over the years to keep the turbine airfoils temperatures below critical levels consistent with the required life for each component. Parallel with advances in airfoil material properties, advances in airfoil cooling schemes have also been remarkable. A main objective in turbine airfoil cooling design is to achieve maximum heat removal from the airfoil metal while minimizing the required coolant flow rate. One such method is to route coolant air through serpentine passages within the airfoil and convectively remove heat from the airfoil. The coolant is then ejected either at the tip of the airfoil, through the cooling slots along the trailing edge or the film holes on the airfoil surface at critical locations. To further enhance the heat transfer, the cooling channel walls are often roughened with ribs. Extensive research has been conducted on various aspects of the rib-roughened channels and it is concluded that geometric parameters such as passage aspect ratio ( $AR$ ), rib height to passage hydraulic diameter or blockage ratio ( $e/D_h$ ), rib angle of attack ( $\alpha$ ), the manner in which the ribs are positioned relative to one another (in-line, staggered, crisscross, etc.), rib pitch-to-height ratio ( $S/e$ ) and rib shape (round versus sharp corners, fillets, rib aspect ratio ( $AR_{rib}$ ), and skewness towards the flow direction) have pronounced effects on both local and overall heat transfer coefficients. The interested reader is referred to the work of investigators such as Burggraf [1], Chandra and Han [2], El-Husayni et al. [3], Han [4], Han et al. [5, 6, 7], Metzger et al. [8, 9, 10], Taslim and Spring [11, 12], Taslim et al. [13, 14, 15], Webb et al. [16] and Zhang et al. [17].

Airfoil leading-edge surface, being exposed to very high gas temperatures, is often a life-limiting region and requires more complex cooling schemes especially in modern gas turbines with elevated turbine inlet temperatures. A combination of convective and film cooling is used in conventional designs to maintain the leading-edge metal temperature at levels consistent with airfoil design life. This study focuses on the leading-edge jet impingement and effects that roughening of the leading-edge surface has on the impingement heat transfer coefficient. In this flow arrangement, the coolant enters the leading-edge cooling cavity as jets from the adjacent cavity through a series of crossover holes on the partition wall between the two cavities. The cross-over jets impinge on the leading-edge wall and exit through the leading-edge film holes on the pressure and suction sides, or form a crossflow in the leading-edge cavity and move toward the airfoil tip. A survey of many existing gas turbine airfoil geometries show that, for analytical as well as experimental analyses, such cavities can be simplified by simulating the shape as a four-sided polygon with one curved side that simulates the leading edge curvature, a rectangle with one curved side (often the smaller side) or a trapezoid, the smaller base of which is replaced with a curved wall. The available data in open literature is mostly for the jet impingement on flat surfaces that are smooth or rib-roughened and a few cases of impingement on concave but smooth surfaces. These studies include the work of Chupp et al. [18], Metzger et al. [19], Kercher and Tabakoff [20], Florschütz, et al. [21, 22, 23], Metzger and Bunker [24], Bunker and Metzger [25], Van Treuren et al. [26], Chang et al. [27], Huang et al. [28], and Akella and Han [29]. However, as dictated by the external shape of an airfoil leading edge, the test section in this investigation was a symmetric channel with a circular nose, two tapered side walls and a flat fourth wall on which the crossover jets were positioned. Experimental results for this setup with circular crossover holes have already been reported by Taslim et al. [30]. The present study, however, deals with the impingement of racetrack-shaped crossover jets, at  $0^\circ$  and  $45^\circ$  angles with the cooling channel's radial axis,  $\gamma$ , on a smooth as well as roughened target surface. Depending on the flow arrangement, the impingement air was ejected entirely through a row of holes on the target surface along the leading edge simulating the airfoil showerhead film holes, or split through the showerhead holes and two rows of holes on the side walls representing the pressure and suction side "gill" film holes, or partially (70%) through the showerhead holes and the balance (30%) through one end of the channel representing an airfoil tip. Data were gathered for a range of jet Reynolds number up to 20000 and were compared with those of circular impinging jets.

## TEST SECTIONS

Figures 1 and 2 show schematically the layout, cross-sectional area, and the target surface geometries for the four test sections investigated in this project. A conventional technique of heated walls in conjunction with thermocouples was used to measure the heat transfer coefficient.

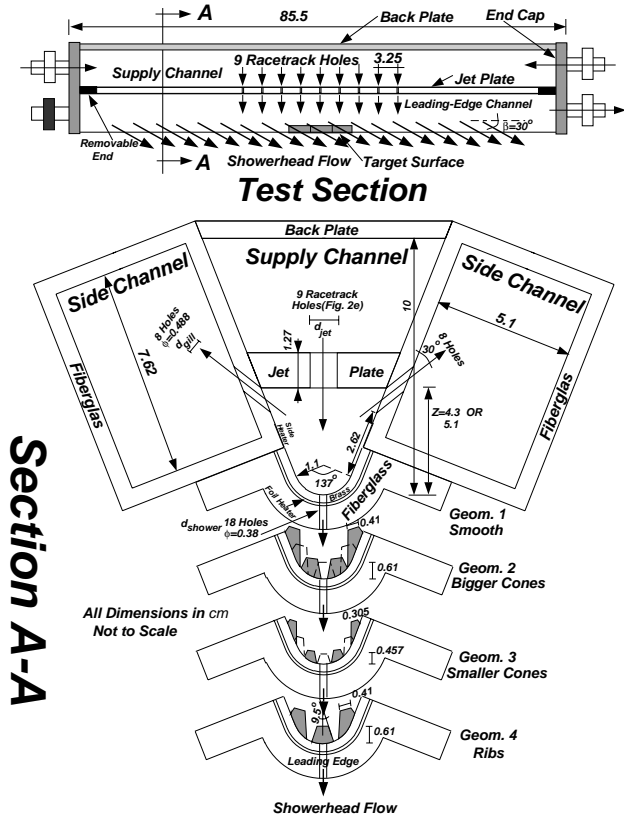


Figure 1 Schematic of the test apparatus.

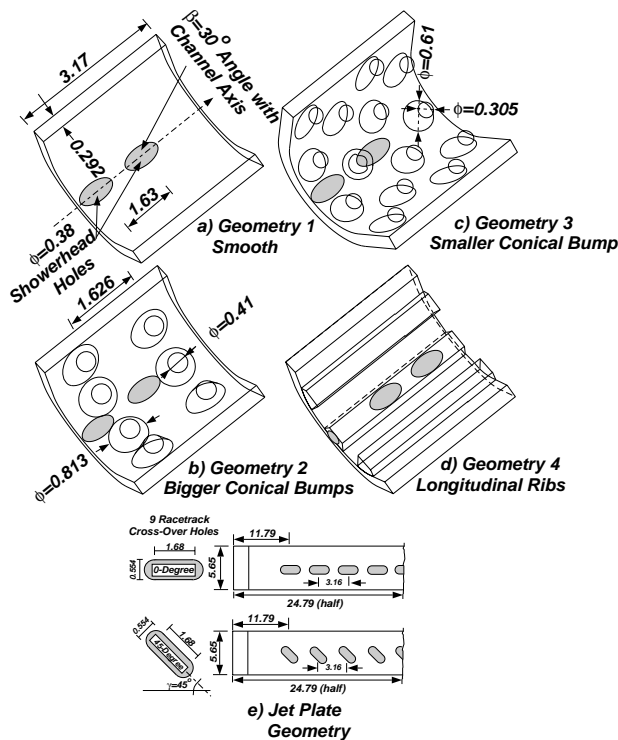
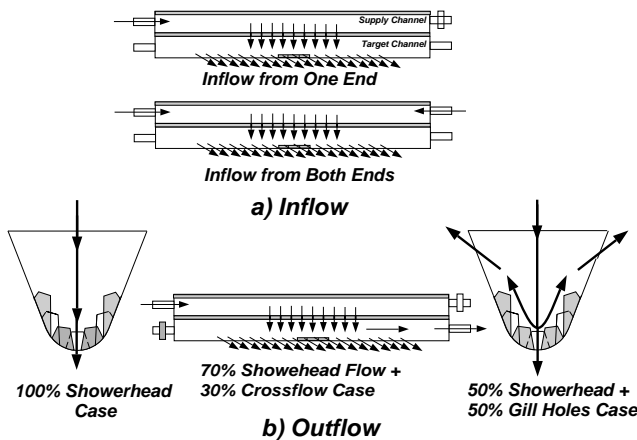


Figure 2 Target surface and crossover jet geometries.

The test wall, where all measurements were taken, consisted of three removable cast brass pieces which were heated by foil heaters attached on the back of the pieces. By proper adjustment of the ohmic power to the foil heater immediately underneath the brass piece, the desirable surface temperature was obtained. All test sections were 85.5 cm long. The circular wall simulating the leading-edge nose with an inner radius of 1.1 cm and an arc angle of  $137^\circ$  was made of fiberglass with a 9.9 cm long recess in the middle to house the three brass pieces. Eighteen 0.38-cm- diameter holes at a center-to-center distance of 1.63 cm were drilled along the leading edge nose at a  $30^\circ$  angle with the channel longitudinal axis. Six of these holes passed through the brass pieces while the rest were drilled symmetrically on both sides of the brass pieces on the fiberglass nose. This single row of holes, with properly scaled flow area, simulated an airfoil showerhead hole design that is typically configured as two rows. This test rig, however, was limited to one row of holes because the brass pieces were covered with etched-foil heaters through which could not be drilled. A flange on each side of the leading-edge piece facilitated the connection of the side walls to this piece. A circular recess along the inner radius with a depth of 3.2 mm and a length of 9.9 cm allowed the brass pieces to be fitted into the fiberglass shell. The two identical side channels with cross-sectional areas of 38.86 cm<sup>2</sup> (5.1 cm by 7.62 cm) and the same length as the leading-edge piece were also made of fiberglass. The side channels' main function was to maintain the dump pressure to consequently control the amount of flow through the "gill" holes on the airfoil suction and pressure sides. Eight angled cylindrical holes with a diameter of 4.88 mm and a center-to-center distance of 3.25 cm were drilled on each side channel wall at an angle of  $30^\circ$  with the side wall to simulate gill holes on the suction and pressure sides of an airfoil. These holes were staggered along the length of the test section with respect to the crossover jet holes on the jet plate.

Four removable 1.27 cm thick jet plates corresponding to two values of  $Z/d_{jet}=4.65$  and 5.5 and two jet angles,  $\gamma$ , with respect to the cooling channel's longitudinal axis of  $0^\circ$  and  $45^\circ$ , were made of acrylic plastic to produce the impinging jets (Figure 2e). Nine racetrack-shaped holes with a cross section shown in Figure 2e were drilled at a distance of 3.16 cm from each other (center-to-center) on each jet plate. For each  $Z/d_{jet}$  test, the corresponding jet plate was attached and sealed to the side channel walls to simulate the partition wall between the leading-edge and its adjacent cooling cavity in an airfoil. The crossover holes were centered with respect to both the length and width of the jet plate. For the nominal position of the jet plate, a jet impinged at the center of each brass piece. To be able to move the impinging jets to an off-center position, two removable 0.82 cm thick pieces were attached to each end of the jet plates to allow three different impingement locations. The removable brass pieces, installed in the fiberglass outer shell, provided the ability to change the impingement surface geometries in the test rig. Four different geometries were manufactured and tested (Figure 2): (1) a smooth wall that served as a baseline,



**Figure 3 Inflow and outflow arrangements.**

(2) a roughened wall with seven conical bumps on each brass piece, (3) a roughened wall with fourteen smaller conical bumps on each brass piece, (4) a roughened wall with tapered radial ribs.

For each geometry, a Unigraphics<sup>R</sup> model was created and transmitted to the manufacturer electronically, and a LOM (Laminated Object Model) was made. This LOM model was used to mold and eventually create a cast brass test piece for each of the four geometries. Two 3 cm by 3.1 cm custom-made thin etched-foil heaters with a thickness of about 0.2 mm were glued around the outer surface of each brass piece to provide the necessary heat flux. For each geometry, three identical brass pieces, separated by a 1 mm thick rubber insulator, were mounted next to each other. Heat transfer coefficients were measured on the middle piece while the other two pieces acted as guard heaters to minimize the heat losses to the adjacent walls. In addition, two custom-made thin etched-foil heaters were mounted on the test section side channel walls next to the middle brass piece free edges, again acting as guard heaters. The test section wall temperature was adjusted to a desirable level by varying the ohmic power to these heaters. Six thermocouples were embedded in the middle brass piece with their beads close to the exposed surface. Two of these thermocouples were drilled into the surface roughnesses. Three thermocouples were embedded in each guard brass piece. The average of the six thermocouple readings in the middle brass piece, which, if different, only differed by a fraction of a degree, was used as the surface temperature in the data reduction software for the average heat transfer coefficient. A nominal surface temperature of 45°C was selected so that with a jet temperature of about 20°C, a reasonable 25°C temperature difference existed between the wall surface and air. Two thermocouples embedded in the wall behind the guard heaters were used to measure the wall temperature adjacent to the middle brass piece. By proper adjustment of the power to the side heaters, the wall temperature under the side heaters was set to be around 45°C. AC power was supplied to individual heaters through an existing power panel with individ-

ual Variacs for each heater. Typical amperage and voltage levels for each heater varied from 0.23 - 0.4 Amps and 20-45 Volts, respectively. Air properties were evaluated at jet temperature.

The trapezoidal supply channel was formed by the exterior walls of the side channels, the jet plate and a 1.27 cm thick aluminum back plate as shown in Figure 1. The end caps were fixed such that it was possible to control the flow and pressure in each channel, thus simulating many variations that may occur in actual airfoil environments. Static pressure taps and thermocouples in each channel measured the pressure and temperature at different locations. The test sections were covered on all sides, by 5 cm thick glasswool sheets to minimize heat losses to the environment. More details of the geometry and test results are reported in Pan [31] radiational heat loss from the heated wall to the unheated walls, heat losses from the brass piece in the entrance region of the showerhead holes, and losses to ambient air were taken into consideration when heat transfer coefficients were calculated. A contact micromanometer with an accuracy of 0.025 mm of water column as well as a series of oil and mercury manometers measured the pressures and pressure differences between the static pressure taps mounted on both sides of the roughened section for each geometry. For all cases, a critical venturimeter was used to measure the total air mass flow rate entering the supply channel.

## RESULTS AND DISCUSSION

A total of 96 tests were run in this investigation. All tests had several common features. There were always nine impinging jets issuing from the jet plate. The middle jet (*fifth*) always impinged on the brass test piece in the middle of the test section and the reported heat transfer results are always for that middle brass test piece. Heat losses from the middle brass piece to the ambient by conduction and convection as well as the heat losses by radiation to the unheated walls were taken into consideration when the impingement heat transfer coefficient was calculated. The fourth and sixth jets impinged on the side brass pieces that acted as guard heaters. The remaining six jets impinged on the fiberglass leading-edge wall to simulate the flow field in a typical leading-edge cooling channel. The jet Reynolds number is based on the total measured mass flow rate and the total area of the nine impingement holes. Two inflow arrangements to the supply channel, as shown in Figure 3a, where air either entered from one end or both ends, were tested. Static pressure taps, installed in the middle and at each end of the supply channel, measured no significant difference between locations (about 1 cm of water column for a supply pressure ranging from 110 to 172 KPa). Three outflow arrangements for the exiting cooling air, shown in Figure 3b, were tested. The "100% showerhead flow" case was the case in which all cooling air, after impinging on the leading-edge wall, was ejected through a row of holes on the target surface. The "50% showerhead flow" case was the case in

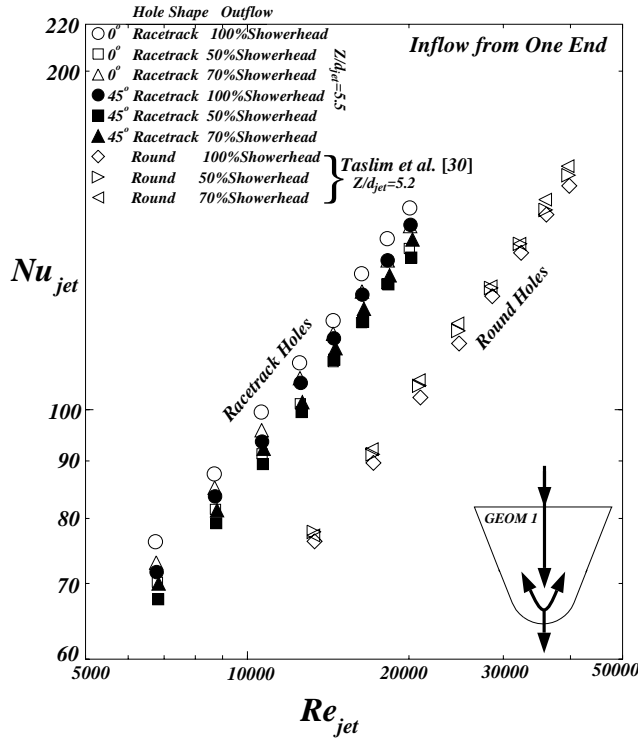


Figure 4 Comparison between the results of racetrack-shaped and round crossover jets impinging on target surface geometry 1 (smooth).

which 50% of the cooling air, after impinging on the leading-edge wall, was ejected through the leading-edge holes and the remaining 50% through the side holes simulating the “gill” holes on the pressure and suction sides of an airfoil. The “70% shower+crossflow” case was the case in which 70% of the cooling air, after impinging on the leading-edge wall, was ejected through the leading-edge holes while the remaining 30% was ejected from one end of the leading-edge channel simulating the airfoil tip flow. In this flow arrangement, portion of the four jets upstream of the middle jet that was not ejected through the leading-edge holes (spent air) formed a crossflow that affected the impingement heat transfer coefficient. Two jet plate positions corresponding to  $Z/d_{jet}$  values of 4.65 and 5.5 were tested for all geometries. Specific characteristics of each geometry are discussed next. Experimental uncertainty in heat transfer coefficient, following the method of Kline and McClintock [32] was determined to be 6%.

### Geometry 1

Impingement on a smooth leading-edge wall, shown in Figure 2a, was tested in this study to serve as a baseline geometry. Figure 4 compares the heat transfer results of racetrack-shaped crossover holes with those of round impinging jets that have been reported previously (Taslim et al. [30]). The relative jet distances to the target surface,  $Z/d_{jet}$ , were 5.2 and 5.5 for the round and racetrack

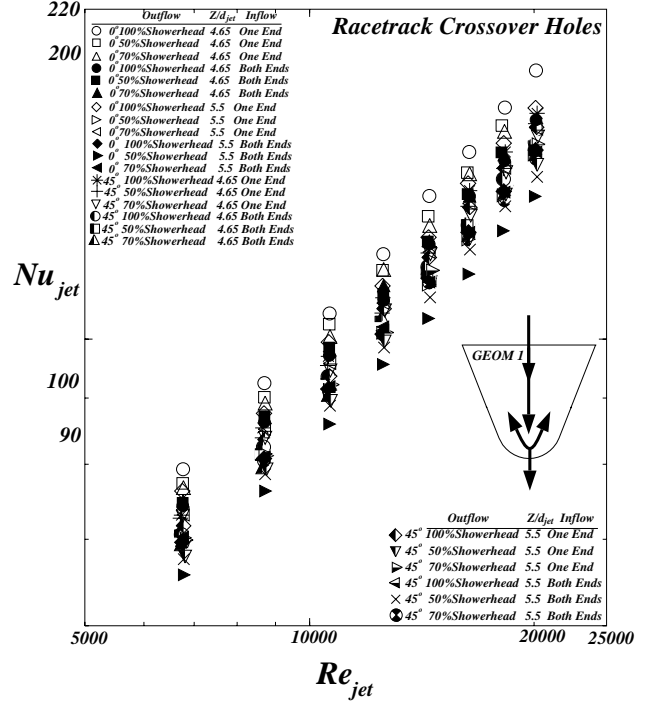


Figure 5 Comparison between 0 and 45 degree racetrack crossover hole results for geometry 1 (smooth wall).

holes, respectively, and the cooling air entered the supply channel from one end in both cases. It can be seen that, for a given jet Reynolds number, racetrack holes of both 0 and 45 degrees produced higher Nusselt numbers ranging from a maximum difference of about 50% (between the 100% Showerhead cases of round jets and 0° racetrack-shaped jets) to a minimum of about 28% (for the 50% Showerhead outflow arrangements of round jets and 45° racetrack-shaped jets). This behavior was also reported (Taslim and Setayeshgar [33]) for jet impingement on the leading-edge surface without the showerhead holes. It should be noted that, for a matching jet Reynolds number, the coolant mass flow rate through the racetrack holes was about twice as much of that for the round holes (mass flow rate ratio is equal to the ratio of crossover hole perimeters). A physical explanation for this increase is that for a given jet Reynolds number, although the round jets had a higher impingement velocity (about 12% higher), the racetrack jets had a combination of higher coolant mass flow rates and better coverage of the target surface. The difference between the round and racetrack-shaped jet results remains almost the same with the jet Reynolds number but it varies across the target surface geometries, as we will discuss later. If this comparison is done for identical coolant mass flow rates, then the jet Reynolds numbers for the round holes would be 1.98 times the racetrack hole Reynolds numbers which result in slightly higher Nusselt numbers for the round jets. However, to make the results useful for different geometries and flow applications, they are presented in terms of pertinent non-dimensional parameters.

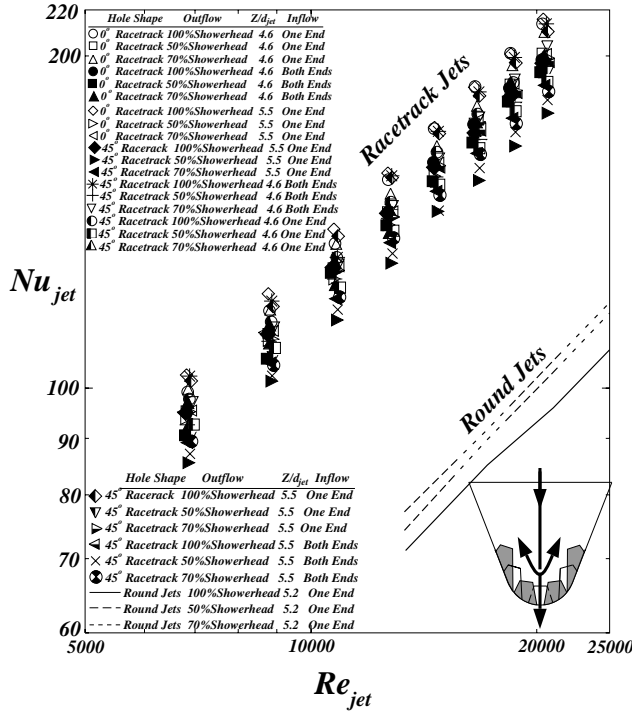


Figure 6 Comparison between 0 and 45 degree racetrack crossover hole results for geometry 2 (bigger cones).

Figure 5 shows the results of all tests performed on the smooth target surface geometry for the two racetrack hole angles each for two  $Z/d_{jet}$  values and for two inflow and three outflow conditions. Zero-degree racetrack holes at the shortest distance to the target surface produced the highest impingement heat transfer coefficients when the cooling air was totally ejected through the showerhead film holes while the the same racetrack holes at the higher  $Z/d_{jet}$  produced the lowest heat transfer results when the cooling jets were split between the showerhead and gill holes. Other general observations are (a) smaller  $Z/d_{jet}$  values produced higher heat transfer coefficients for both racetrack crossover hole angles which is attributed to less diffusion of the jets and more effective impingement on the target surface, (b) the 0° racetrack jets are more effective than 45° racetrack jets for all inflow and outflow arrangements indicating that the more symmetric 0° racetrack jets come in a better contact with the target surface, and cover more of it while departing, than the 45° racetrack jets, (c) under otherwise identical conditions, flow entering the supply channel from one end (Fig. 3a top) produced higher heat transfer coefficients. This behavior is attributed to a slightly higher share of the total mass flow for the fifth jet for which the heat transfer results are reported. The flow distribution for the nine crossover holes when flow enters from one end or both ends of the supply channel is shown in Taslim et. al [34] and is not repeated here, and d) 100% showerhead outflow cases, in general, produced higher impingement heat transfer coefficients compared to the other two outflow arrangements. A physical explanation for this behavior is that when the impinging jet hits the target

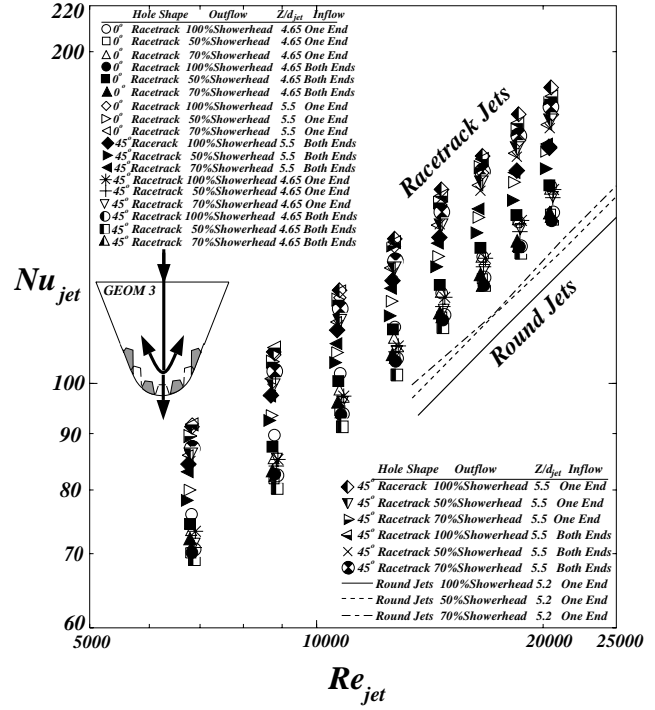


Figure 7 Comparison between 0 and 45 degree racetrack crossover hole results for geometry 3 (smaller cones).

surface directly and exits, by its entirety, through the showerhead holes on that target surface, it is more effective than having to split into three streams two of which are exited through the gill holes without an effective interaction with the target surface.

## Geometry 2

The target wall for this geometry was roughened with the bigger conical bumps (Figure 2b). This configuration consisted of a total of fourteen conical bumps on each brass piece made up in four staggered rows of three and four cones each. Compared to the baseline geometry, the total heat transfer area on the middle brass piece was increased by about 35%. Figure 6 shows the results of all tests performed on this target surface geometry for two racetrack hole angles, each for two  $Z/d_{jet}$  values, and each for two inflow and three outflow conditions. Representative round jet results are also shown to indicate the superiority of racetrack crossover holes in leading-edge impingement cooling. The difference between the round and racetrack jets is much more than the baseline case (a two-fold increase at its maximum) indicating that the racetrack jets came in a much better contact with the extended areas of the conical bumps. 0° racetrack jets, when they were ejected entirely through the showerhead holes, produced the highest impingement heat transfer coefficients while the same jets, when they exited equally through the showerhead and gill holes, produced the lowest impingement heat transfer coefficients. Maximum difference between these two cases is about 20%. Similar to

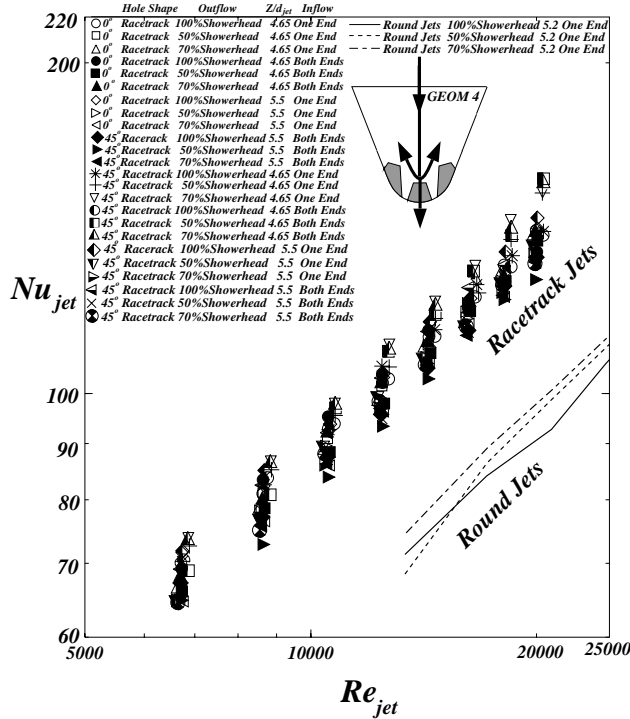


Figure 8 Comparison between 0 and 45 degree racetrack crossover hole results for geometry 4 (ribs).

the baseline geometry, the 100% showerhead flow cases produced higher heat transfer coefficients than the two other outflow arrangements. The 0° racetrack holes in all flow cases performed better than 45° angles. This behavior was also observed in our previously reported study (Taslim and Setayeshgar [33]) on racetrack jet impingement without showerhead holes. When the racetrack jets are tilted, part of the cooling air may not interact with the conical bumps which could result in lower heat transfer coefficients.

Similar to the results of our previous studies on this subject, the dominant parameter in heat transfer enhancement with impingement on roughened surfaces is the area increase. Geometry comparisons are done in ensuing Figures 9 through 11 in which the heat transfer coefficients on the three target surface geometries as well as the area-enhanced heat transfer [ $Nu_{jet}(A_{HT}/A_{base})$ ] are compared and discussed.

### Geometry 3

Geometry 3 (Figure 2c) was made of smaller conical bumps but more in number. This configuration consisted of a total of fourteen conical bumps made up in four staggered rows of four and three cones each. Compared to the baseline geometry, the total heat transfer area on the middle brass piece was again increased by about 35%. A total of twenty four tests were run for this geometry to cover the three outflow cases (100% showerhead, 50% showerhead, 70%

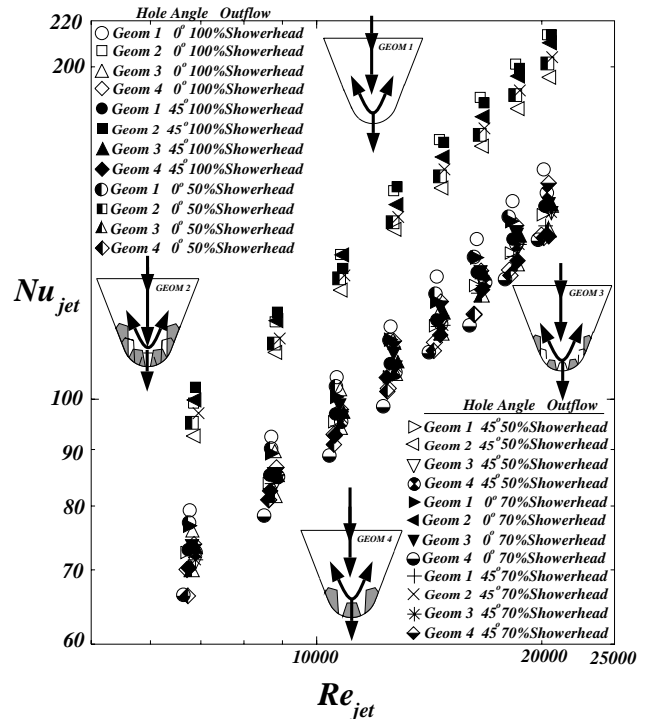


Figure 9 Comparison between different target surface geometries at  $Z/d_{jet}=4.65$  and inflow from one end of the supply channel.

showerhead+crossflow), the two  $Z/d_{jet}$  values of 4.65 and 5.5, and the two racetrack hole angles, the results of which are shown in Figure 7 along with the results of the same geometry with round crossover holes. The results show that compared to geometry 2, this target surface geometry produced lower impingement heat transfer coefficients. A thorough comparison between different geometries is done in the comparison section. It is also observed that the difference between the round and racetrack jet results is not as high as the other two geometries. Depending on the inflow and outflow arrangements, and racetrack jet angle, the difference varies between 1% and 45%. For all flow arrangements and both racetrack jet angles, the difference between the maximum and minimum impingement heat transfer coefficients for this geometry was about 30%.

### Geometry 4

The target wall for this geometry was roughened with longitudinal ribs (Figure 2d). There were three ribs along each brass piece, one on the leading-edge nose and one on each side, parallel to the middle one. The total heat transfer area on the middle brass piece was measured to be 47.3% higher than that of the baseline geometry. Similar to other target surface geometries, a total of twenty four tests were run to cover the three outflow cases, the two  $Z/d_{jet}$  values, and the two racetrack hole angles. The results are shown in Figure 8 along with representative round jet results to show

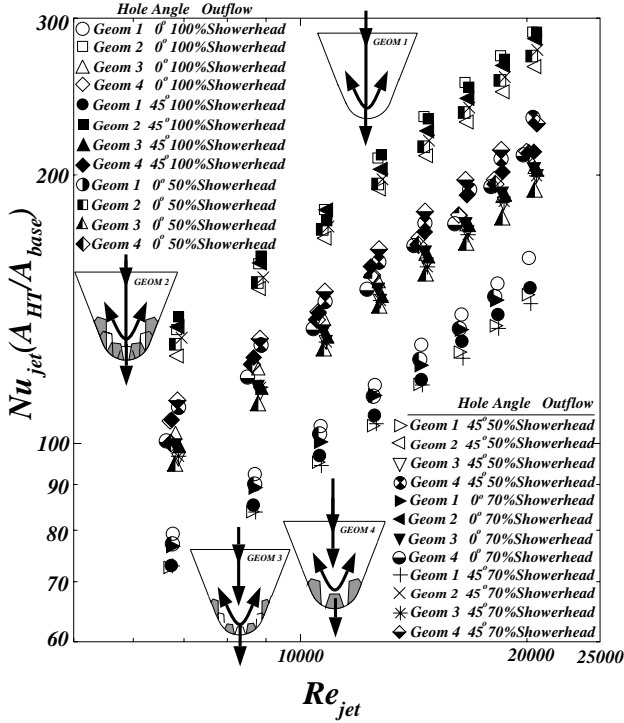


Figure 10 Area-augmented heat transfer results for all geometries at  $Z/d_{jet}=4.65$  and inflow from one end of the supply channel.

the superiority of racetrack crossover holes in impingement on this target surface geometry as well. Compared to the target surface geometries 2 and 3, the longitudinal ribs did not perform as well, neither for round nor for racetrack jets. The same trend was reported in our three previous studies of this geometry (Taslim et al. [30,33,34]) with and without showerhead holes, and round as well as racetrack crossover holes. It appears that the coolant air did not come in a good contact with all available heat transfer areas around the ribs particularly the outermost surfaces. Only when a crossover exists, a slight improvement is observed. Also, the racetrack crossover jets, in general, and the  $45^\circ$  ones, in particular, did somewhat improve this shortcoming of geometry 4. However, the overall performance of the rib-roughened target surface was inferior to that of cone-roughened surfaces. Test results of geometry 4 are also compared with those of other two geometries in Figures 9 through 11 for the two values of  $Z/d_{jet}$ .

### Comparisons

Figures 9 through 11 compare the heat transfer results of all four target surface geometries. The results of  $Z/d_{jet}=4.65$  are compared in Figure 9. The cluster of data points, representing the higher impingement heat transfer levels, belong to the target surface geometry 2 (bigger cones). The lowest heat transfer coefficient is produced by the longitudinal ribs (geometry 4) while the baseline geometry (smooth target sur-

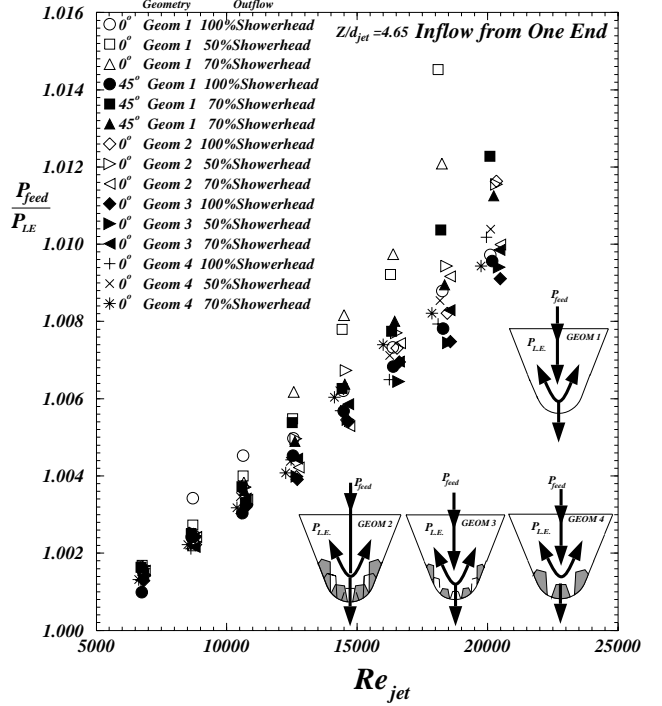


Figure 11 Comparison between the pressure ratios across the jet plates with racetrack-shaped crossover holes for the four target surface geometries.

face) and the small-cone surface (geometry 3) produced comparable results. There exists a maximum difference of about 50%, between the results of geometries 2 and 4. More importantly, the impingement heat transfer coefficient on the cone-roughened target surface (geometry 2) is at least 30% higher than that on the baseline target surface. This is attributed to the combined effects of showerhead holes and racetrack crossover holes since our previous studies that dealt with the same target surface geometries but no showerhead holes (or with showerhead holes but round crossover jets) showed that the roughening of the target surface did not increase the impingement heat transfer coefficient significantly and any benefit from the roughening was in the heat transfer area increase. It appears that the showerhead holes draw the jets to the bottom of the valleys around the cones causing more interaction between the coolant air and the cones, and the racetrack shape of the jets spreads the cooling air over a wider target surface. When this increase in the heat transfer coefficient is added to the increase in the heat transfer area, the end result could be a benefit of up to 75% as is shown in Figure 10. Cross geometry comparisons for the case of inflow from both ends and the second  $Z/d_{jet}$  (5.5) showed the same behavior thus are not presented here due to space limitations.

Figure 10 includes the contribution of the increased area in the overall heat transfer from the target surface [ $Nu_{jet}(A_{HT}/A_{base})$ ] in the data reported in Figure 9. The lower cluster of data represent the baseline geometry while the



bigger cones represent the highest area-augmented heat transfer. The other two target surface geometries still represent a 40 to 45% increase compared to the baseline geometry which is slightly over the increase in their heat transfer area.

Static pressure ratios across the jet plate for all geometries and representative flow arrangements are shown in Figure 11. Several observations are made. At the lower Reynolds number range, different geometries and flow arrangements have almost the same pressure ratios across the jet plate. At higher Reynolds numbers, however, a difference in pressure ratios across the jet plates for different geometries is observed. Higher pressure ratios which did not go beyond 1.016, in general, correspond to the case of a flow split between the showerhead and gill holes. The small difference between the pressure ratios were mainly due to different inflow and outflow arrangements and not to target surface geometry.

## CONCLUSIONS

For a given jet Reynolds number, the racetrack crossover holes produce higher impingement heat transfer coefficients when compared with the round crossover jets. Without the inclusion of the heat transfer area increase, the smaller conical bumps, the longitudinal ribs and the smooth target surface produced comparable results while the bigger cones produced higher impingement heat transfer coefficients by about 30%. When the contribution of the increased area in the overall heat transfer is taken into consideration, geometry 2 for all inflow and outflow cases as well as the two  $Z/d_{jet}$  values proved to be the most effective geometry. An overall increase of up to 75% in heat removal from the target surface can be accomplished by roughening the leading-edge wall with conical bumps. This enhancement for the other two roughened target surface geometry were almost entirely attributed to the increase in their heat transfer area.

## REFERENCES

- [1] Burggraf, F., 1970, "Experimental Heat Transfer and Pressure Drop with Two Dimensional Turbulence Promoters Applied to Two Opposite Walls of a Square Tube," *ASME, Augmentation of Convective Heat and Mass Transfer*, Edited by A.E. Bergles and R.L. Webb, pp. 70-79.
- [2] Chandra, P.R. and Han, J.C., 1989, "Pressure Drop and Mass Transfer in Two-Pass Ribbed Channels", *J. of Thermophysics*, Vol. 3, No. 3, pp. 315-319.
- [3] El-Husayni, H.A., Taslim, M.E., and Kercher, D.M., 1994, "An Experimental Investigation of Heat Transfer Coefficients in a Spanwise Rotating Channel With Two Opposite Rib-Roughened Walls," *J. Turbomachinery*, Vol. 113, pp. 75-82.
- [4] Han, J.C., 1984, "Heat Transfer and Friction in Channels with Two Opposite Rib-Roughened Walls," *J. Heat Transfer*, Vol. 106, No. 4, pp. 774-781.
- [5] Han, J.C., Glicksman, L.R., and Rohsenow, W.M., 1978, "An Investigation of Heat Transfer and Friction for Rib Roughened Surfaces," *Int. J. Heat and Mass Transfer*, Vol. 21, pp. 1143-1156.
- [6] Han, J.C., Park, J.S., and Lei, C.K., 1985, "Heat Transfer Enhancement in Channels With Turbulence Promoters," *J. of Engineering For Gas Turbines and Power*, Vol. 107, No. 1, pp. 628-635.
- [7] Han, J.C., Zhang, Y.M., and Lee, C.P., 1992, "Influence of Surface Heat Flux Ratio on Heat Transfer Augmentation in Square Channels with Parallel, Crossed, and V-shaped Angled Ribs," *J. Turbomachinery*, Vol. 114, pp. 872-880.
- [8] Metzger, D.E., Vedula, R.P., and Breen, D.D., 1987, "The Effect of Rib Angle and Length on Convection Heat Transfer in Rib-Roughened Triangular Ducts," *Proceedings of the ASME-JSME Thermal Engineering Joint Conference*, Vol. 3, pp. 327-333.
- [9] Metzger, D.E., Chyu, M.K. and Bunker, R.S., 1988, "The Contribution of On-Rib Heat Transfer Coefficients to Total Heat Transfer from Rib-Roughened Surfaces," *Transport Phenomena in Rotating Machinery*, Edited by J.H. Kim, Hemisphere Publishing Co.
- [10] Metzger, D.E., Fan, C.S., and Yu, Y., 1990, "Effects of Rib Angle and Orientation on Local Heat Transfer in Square Channels with Angled Roughness Ribs," *Compact Heat Exchangers : A Festschrift for A.L. London*, Hemisphere Publishing Co., pp. 151-167.
- [11] Taslim, M.E. and Spring, S.D., 1988, "An Experimental Investigation of Heat Transfer Coefficients and Friction Factors in Passages of Different Aspect Ratios Roughened With 45° Turbulators," *Proc. National Heat Conference*, Houston, TX.
- [12] Taslim, M.E. and Spring, S.D., 1988, "Experimental Heat Transfer and Friction Factors in Turbulated Cooling Passages of Different Aspect Ratios, Where Turbulators are Staggered," *Paper AIAA-88-3014*.
- [13] Taslim, M.E., Bondi, L.A., and Kercher, D.M., 1991, "An Experimental Investigation of Heat Transfer in an Orthogonally Rotating Channel Roughened 45 Degree Criss-Cross Ribs on Two Opposite Walls," *J. of Turbomachinery*, Vol. 113, pp. 346-353.
- [14] Taslim, M.E. and Spring, S.D., 1991, "An Experimental

Investigation into the Effects Turbulator Profile and Spacing Have on Heat Transfer Coefficients and Friction Factors in Small Cooled Turbine Airfoils," *Paper # AIAA-91-2033*.

[15] Taslim, M.E., Rahman, A. and Spring, S.D., 1991, "An Experimental Investigation of Heat Transfer Coefficients in a Spanwise Rotating Channel With Two Opposite Rib- Roughened Walls," *J. of Turbomachinery*, Vol. 113, pp. 75-82.

[16] Webb, R.L., Eckert, E.R.G. and Goldstein, R.J., 1971, "Heat Transfer and Friction in Tubes with Repeated-Rib-Roughness," *Int. J. Heat Mass Transfer*, Vol. 14, pp. 601-617.

[17] Zhang, Y.M., Gu, W.Z. and Han, J.C., 1994, "Heat Transfer and Friction in Rectangular Channels with Ribbed or Ribbed-Grooved Walls," *J. Heat Transfer*, Vol. 116, No. 1, pp. 58-65.

[18] Chupp, R.E., Helms, H.E., McFadden, P.W., and Brown, T.R., 1969, "Evaluation of Internal Heat Transfer Coefficients for Impingement Cooled Turbine Blades," *J. Aircraft*, Vol. 6, No. 1, pp. 203-208.

[19] Metzger, D.E., Yamashita, T. and Jenkins, C.W., 1969, "Impingement Cooling of Concave Surfaces With Lines of Circular Air Jets," *J. Engr. for Power*, Vol. 93, No. 3, pp. 149-155.

[20] Kercher, D.M. and Tabakoff, W., 1970, "Heat Transfer by a Square Array of Round Air Jets Impinging Perpendicular to a Flat Surface Including the Effect of Spent Air," *J. Engr. for Power*, Vol. 92, No. 1, pp. 73-82.

[21] Florschetz, L.W., Berry, R.A., and Metzger, D.E., 1980, "Periodic Streamwise Variation of Heat Transfer Coefficients for Inline and Staggered of Circular Jets with Crossflow of Spent Air," *J. Heat Transfer*, Vol. 102, No. 1, pp. 132-137.

[22] Florschetz, L.W., Truman, C.R., and Metzger, D.E., 1981, "Streamwise Flow and Heat Transfer Distribution for Jet Impingement with Crossflow," *J. Heat Transfer*, Vol. 103, No. 2, pp. 337-342.

[23] Florschetz, L.W., Metzger, D.E., Su, C.C., Isoda, Y., and Tseng, H.H., 1984, "Heat Transfer Characteristics for Jet Arrays Impingement with Initial Crossflow," *J. Heat Transfer*, Vol. 106, No. 1, pp. 34-41.

[24] Metzger, D.E., and Bunker, R.S., 1990, "Local Heat Transfer in Internally Cooled Turbine Airfoil Leading Edge Regions: Part I - Impingement Cooling Without Film Coolant Extraction," *J. Turbomachinery*, Vol. 112, No. 3, pp. 451-458.

25] Bunker, R.S., and Metzger, D.E., 1990, "Local Heat Transfer in Internally Cooled Turbine Airfoil Leading Edge Regions: Part II - Impingement Cooling With Film Coolant Extraction," *J. Turbomachinery*, Vol. 112, No. 3, pp. 459-466.

[26] Van Treuren, K.W., Wang, Z., Ireland, P.T., and Jones, T.V., 1994, "Detailed Measurements of Local Heat Transfer Coefficient and Adiabatic Wall Temperature Beneath an Array of Impinging Jets," *J. of Turbomachinery*, Vol. 116, No. 2, pp. 269-374.

[27] Chang, H., Zhang, D., and Huang, T., 1997, "Impingement Heat Transfer from Rib Roughened Surface Within Arrays of Circular Jet : The Effect of the Relative Position of the jet Hole to the Ribs," *Paper # 97-GT-331*.

[28] Huang, Y., Ekkad, S.V., and Han, J.C., 1998, "Detailed Heat Transfer Distributions Under an Array of Orthogonal Impinging Jets," *J. Thermophysics and Heat Transfer*, Vol. 12, No. 1, pp. 73-79.

[29] Akella, K.V. and Han, J.C., 1999, "Impingement Cooling in Rotating Two-pass Rectangular Channels with Ribbed Walls," *J. Thermophysics and Heat Transfer*, Vol. 13, No. 3, pp. 364-371.

[30] Taslim, M.E., Pan, Y. and Spring, S.D., 2001, "An Experimental Study of Impingement on Roughened Airfoil Leading-Walls with Film Holes," *J. of Turbomachinery*, Vol. 123, No. 4, pp. 766-773.

[31] Pan, Y., 2000, "An Experimental Investigation of an Airfoil Leading-Edge Impingement Cooling with Showerhead Film Holes", *MS Thesis*, Mechanical, Industrial and Manufacturing Engineering Department, Northeastern University, Boston, MA.

[32] Kline, S.J. and McClintock, F.A., 1953, "Describing Uncertainty in Single-Sample Experiments," *Mechanical Engineering*, Vol. 75, Jan., pp. 3-8.

[33] Taslim, M.E. and Setayeshgar, L., 2001, "Experimental Leading-Edge Impingement Cooling Through Racetrack Crossover Holes," *Paper # 2001-GT-0153*.

[34] Taslim, M.E., Setayeshgar, L. and Spring, S.D., 2001, "An Experimental Evaluation of Advanced Leading Edge Impingement Cooling Concepts," *J. of Turbomachinery*, Vol. 123, No. 2, pp. 147-153.